Available online at www.sciencedirect.com
SCIENCE DIRECT®
Journal of Molecular Structure 649 (2003) 207–218
Journal of MOLECULAR STRUCTURE
www.elsevier.com/locate/molstruc

Comparison of epimeric methyl lithocholate and methyl iso-lithocholate molecules: single crystal X-ray structure of methyl lithocholate, ab initio HF/6-31G* optimized structures and experimental and calculated DFT/B3LYP ^{13}C NMR chemical shifts

E. Virtanen*, M. Nissinen, R. Suontamo, J. Tamminen, E. Kolehmainen

Department of Chemistry, University of Jyväskylä, P.O. Box 35, FIN-40014 University of Jyväskylä, Finland

Received 11 June 2002; revised 30 August 2002; accepted 30 August 2002

Abstract

^{13}C NMR chemical shifts have been measured and assigned for epimeric methyl 3α/β-hydroxy-5β-cholan-24-oates (methyl lithocholate [3α-OH epimer] and methyl iso-lithocholate [3β-OH epimer]). Their molecular dynamics simulations suggest that for both epimers there exists two predominant gas phase conformations, which have been further forwarded for ab initio/HF optimizations and DFT/GIAO based ^{13}C NMR chemical shift calculations. Excellent linear relationships have been observed between experimental and calculated ^{13}C NMR chemical shifts for both epimers. For methyl lithocholate (MeLC), the other minimum energy conformation equates very well with the single crystal X-ray structure (orthorhombic, space group $P2_12_12_1$, unit cell $a = 7.14710(10)$ Å, $b = 11.9912(2)$ Å, $c = 26.4368(5)$ Å). The crystalline packing of MeLC consists of continuous parallel intermolecular hydrogen bonded [3α-O**H**···**O**=C24] head-to-tail polymeric chains, which are further cross-linked by many simultaneous weak C(sp^3)**H**···**O**-type of interactions.

Keywords: Methyl 3α-hydroxy-5β-cholan-24-oate; Methyl 3β-hydroxy-5β-cholan-24-oate; X-ray structure; ^{13}C NMR chemical shifts; Ab initio/HF optimized structures; DFT/GIAO

1. Introduction

Mammalian primary bile acids; 3α,7α,12α-trihydroxy-5β-cholan-24-oic acid (cholic acid, CA) and 3α,7α-dihydroxy-5β-cholan-24-oic acid (chenodeoxycholic acid, CDCA) are formed from cholesterol in the liver via multiple enzymatic steps. They are further transformed to secondary bile acids; 3α,12α-dihydroxy-5β-cholan-24-oic acid (deoxycholic acid, DCA) and 3α-hydroxy-5β-cholan-24-oic acid (lithocholic acid, LCA) in the colon [1]. More than 100 bile acid derivatives have been characterized recently by their ^{13}C NMR data [2]. Further, plenty of X-ray structural data for organic inclusion compounds of bile acids (often called choleic acids) have been published [3], while X-ray data for LCA and methyl lithocholeic

* Corresponding author. Tel.: +358-14-260 2654; fax: +358-14-260 2501.
E-mail address: elvirtan@cc.jyu.fi (E. Virtanen).

0022-2860/03/$ - see front matter © 2002 Elsevier Science B.V. All rights reserved.
PII: S0022-2860(02)00476-3

acid (MeLC) are relatively scarce. As far as we know there exists only one paper from 1965 [4], in which the basic crystal data for MeLC (crystallized from ethanol) are given. Full crystal data and structural parameters of LCA (crystallized from acetic acid) have been published in 1976 [5]. In the paper also X-ray dihedral angles of conformationally flexible side chains of LCA, DCA, and CA are compared.

High quality X-ray crystal data are extremely valuable from several points of view, such as (i) for the determination of absolute configuration of bile acids, (ii) for the evaluation of possible intra- and intermolecular weak interactions and self-assembly properties, and (iii) for functioning as starting structures for molecular dynamics simulations and molecular modeling for these conformationally flexible compounds. In addition, DFT/GIAO based calculational methods for optimized structures provide for steroids the theoretical ^{13}C NMR chemical shifts, which are useful in assigning experimental NMR data [6]. In our review article [7] we describe the use of LCA as a building block in several open (steroidal clefts) and cyclic structures (cholaphanes) capable of acting as supramolecular hosts. Further, we have observed that particular ^{13}C NMR chemical shifts of D-ring and side chain of LCA-moiety are sensitive to the steric strain and conformational preferences related to the size of the cholaphane [8]. Therefore, it was interesting to compare the now available high quality single crystal X-ray structural data of MeLC (obtained from a giant single crystal grown by extremely slow evaporation of tetradeuteriomethanol) with the theoretical minimum energy (gas phase) conformations obtained by sophisticated quantum chemical methods. Furthermore, experimental ^{13}C NMR chemical shifts corresponding to the statistical average of solution state conformations of MeLC and its epimeric form, methyl 3β-hydroxy-5β-cholan-24-oate (methyl iso-lithocholate or i-MeLC) are compared with the DFT/GIAO calculated shifts of the optimized conformations. All obtained results will further serve for the interpretation of the spectral data of our forthcoming works on bile acid-derived compounds, their conformational preferences, and molecular recognition properties.

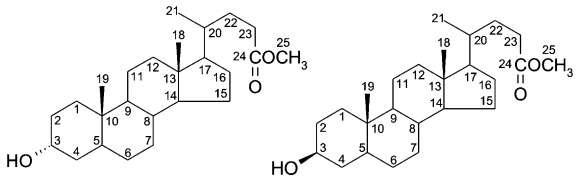

Fig. 1. The structures and numbering of isomeric methyl 3α-hydroxy-5β-cholan-24-oate (methyl lithocholate, MeLC, left) and 3β-hydroxy-5β-cholan-24-oates (methyl iso-lithocholate, i-MeLC, right).

2. Experimental

2.1. Compounds

Methyl lithocholate (MeLC) was prepared by sulphuric acid catalyzed esterification reaction of

Table 1
Crystal data and structure refinement parameters of MeLC

Identification code	CCDC-179240
Empirical formula	$C_{25}H_{42}O_3$
Formula weight	390.59
Temperature	173.0(2) K
Wavelength	0.71073 Å
Crystal system	Orthorhombic
Space group	$P2_12_12_1$ (No. 19)
Unit cell dimensions	$a = 7.14710(10)$ Å, $\alpha = 90°$ $b = 11.9912(2)$ Å, $\beta = 90°$ $c = 26.4368(5)$ Å, $\gamma = 90°$
Volume	2265.69(7) Å^3
Z	4
Density (calculated)	1.145 Mg/m^3
Absorption coefficient	0.073 mm^{-1}
$F(000)$	864
Crystal size	0.50 × 0.30 × 0.10 mm^3
Theta range for data collection	3.52–25.68°.
Index ranges	$0 \le h \le 8$, $0 \le k \le 14$, $0 \le l \le 32$
Reflections collected	2385
Independent reflections	2385 [R(int) = 0.0000]
Completeness to theta = 25.68°	96.1%
Maximum and minimum transmission	0.9928 and 0.9646
Refinement method	Full-matrix least-squares on F^2
Data/restraints/parameters	2385/0/421
Goodness-of-fit on F^2	1.062
Final R indices [$I > 2\sigma(I)$]	$R_1 = 0.0357$, $wR_2 = 0.0757$
R indices (all data)	$R_1 = 0.0451$, $wR_2 = 0.0803$
Absolute structure parameter	−2.3(16)
Largest difference peak and hole	0.157 and −0.119 e. Å^{-3}

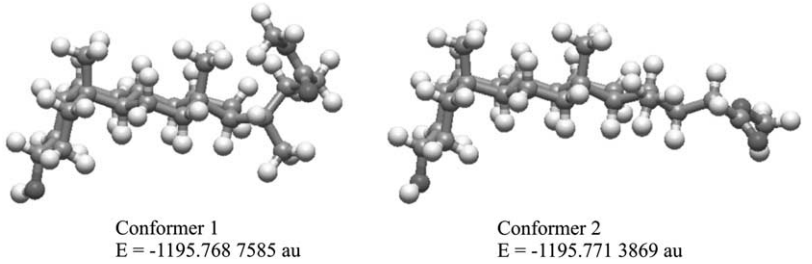

Fig. 2. Ab initio HF/6-31G* optimized structures of MeLC.

LCA (Aldrich, purity > 98%) and excess of methanol as described before [9,10]. Its purity was checked by measuring a ^{13}C NMR spectrum (125.76 MHz), which did not show any impurity signals (spectrum measured both in $CDCl_3$ and in CD_3OD).

i-MeLC was prepared via methyl 3β-formyloxy-5β-cholan-24-oate [11–13], which was synthesized from MeLC by an S_N2 reaction with an inversion of configuration of the 3α-OH group activated by PPh_3/DEAD (diethylazodicarboxylate)-system. The formyl derivative was subsequently cleaved to i-MeLC with 10% sodium methoxide/methanol solution.

Methyl 3β-formyloxy-5β-cholan-24-oate. Reaction was carried out under argon atmosphere. To a solution of MeLC (1.95 g, 5 mmol) and triphenyl phosphine (2.62 g, 10 mmol) in dry THF (60 ml), formic acid (0.46 g, 0.38 ml, 10 mmol) was added. After dropwise addition of a solution of DEAD (1.74 g, 1.58 ml, 10 mmol) in THF (10 ml) stirring was continued overnight at r.t. [12]. Removal of the solvent in vacuo and chromatographic purification on silica gel (toluene/hexane/ethyl acetate 60/40/5) yielded the desired product (1.88 g, 4.49 mmol, 90%). Charact. ^1H NMR at 500 MHz: 7.97 (s, ^1H, HCO), 5.13 (m, ^1H, CH-3α).

Methyl 3β-hydroxy-5β-cholan-24-oate. Methyl 3β-formyloxy-5β-cholan-24-oate (1.88 g, 4.49 mmol) was dissolved in methanol (100 ml) and treated for 24 h with 10% NaOMe/MeOH (70 ml) at r.t. The chilled mixture was acidified (pH 2) with conc. HCl and the solvent was removed in vacuo [13]. The moist crude product was diluted to $CHCl_3$ (2 × 50 ml) and water (1 × 50 ml) and the chloroform layer was separated. Water layer was extracted with $CHCl_3$ (20 ml). Combined $CHCl_3$ layers were dried (Na_2SO_4) and evaporated. Yield: 1.55 g (83%). Charact. ^1H NMR at 500 MHz: 4.00 (m, ^1H, CH-3α).

The structures and numbering of isomeric methyl 3α- and 3β-hydroxy-5β-cholan-24-oates, MeLC (left) and i-MeLC (right), are given in Fig. 1.

2.2. Spectroscopy

All NMR spectra were recorded for 0.1 M solutions in $CDCl_3$ with a Bruker Avance DRX 500 NMR spectrometer equipped with an inverse detection 5 mm diameter probehead and *z*-gradient

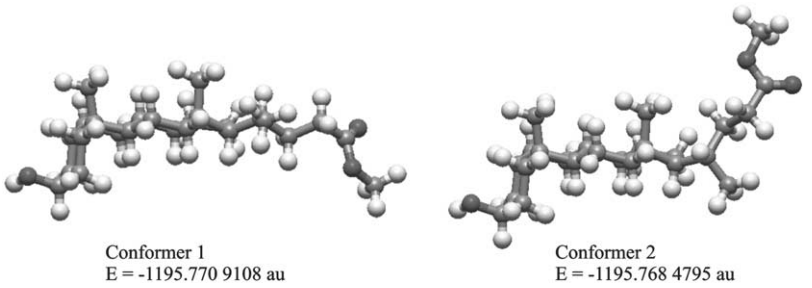

Fig. 3. Ab initio HF/6-31G*optimized structures of i-MeLC.

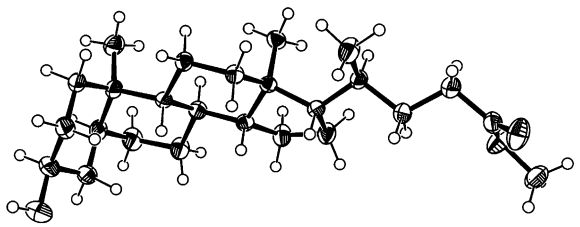

Fig. 4. ORTEP plot of MeLC.

accessory working at 500.13 MHz for proton and 125.76 MHz for carbon-13, respectively.

In ^{1}H NMR experiments, the spectral width was 5000 Hz (10 ppm), the number of data points 65 K, the flip angle 30°, and the number of scans 8. The FIDs were multiplied by an exponential window function of the digital resolution (0.07 Hz) prior to Fourier Transform (FT). The ^{1}H NMR chemical shifts are referenced to the trace signals of $C\mathbf{H}Cl_3$ ($\delta = 7.26$ ppm from TMS) or $CD_2\mathbf{H}OD$ ($\delta = 3.31$ ppm from TMS).

In proton composite pulse decoupled (waltz-16) ^{13}C NMR experiments the spectral width was 25,000 Hz (200 ppm), the number of data points 65 K, the flip angle 30°, and the number of scans 1000. The FIDs were multiplied by an exponential window function of the digital resolution (0.75 Hz) prior to FT. The ^{13}C NMR chemical shifts are referenced to the signal of $\mathbf{C}DCl_3$ ($\delta = 77.00$ ppm from TMS). In ^{13}C DEPT-135 the spectral parameters except of the pulse program were the same as above.

In 2D z-pulsed field gradient (PFG) selected ^{1}H, ^{13}C HMQC [14,15] experiments the acquisition matrix, which was zero filled to 1024×1024 and multiplied by a sine-bell window function along both axes prior to FT, was 2500 Hz/512 points ($^{1}H = f_2$-axis) × 10,000 Hz/512 points ($^{13}C = f_1$-axis). The number of scans was eight and a composite pulse decoupling (garp) was used to remove proton couplings.

2.3. Calculations

Molecular modeling of MeLC was started by optimizing the molecular framework obtained from the crystal structure with HyperChem molecular modeling software [16] using MMI + force field [17,18] molecular mechanics. Molecular dynamics simulations were used in screening the conformational energy space of the molecule in the same force field. In order to locate the possible global energy minima on the potential surface, 10 simulated annealing molecular dynamics runs were performed. Each run started from 0 K, followed by heating for 5 ps to 300 K in temperature steps of 25 K, simulation for 10 ps at 300 K, and cooling for 5 ps close to 0 K, all in time steps of 0.0001 ps. After each simulation the resultant structure was further optimized to 0 K using MMI + force field molecular mechanics. The molecular dynamics simulations and molecular mechanics optimizations for i-MeLC were performed equally. The starting structure was modified from the crystal structure of MeLC. The simulated annealing runs for both epimers led to two conformations, which were further forwarded for semi-empirical PM3 calculations [19].

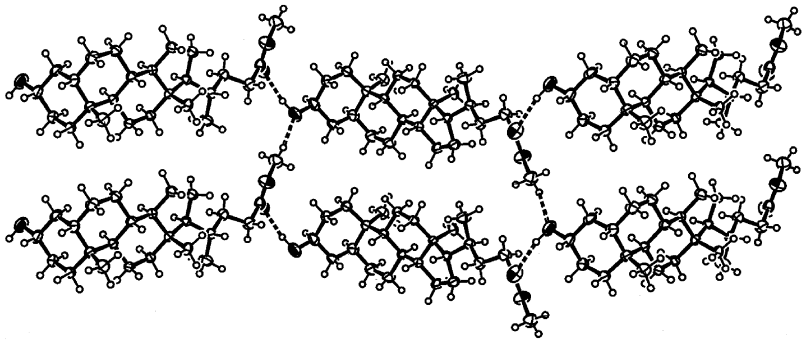

Fig. 5. Crystal packing of MeLC.

Table 2
Calculated (ab initio HF/6-31G*) and experimental (X-ray) bond lengths (Å) for MeLC

Bond length (Å)	Conformer 1	Conformer 2	X-ray structure
C1–C2	1.530	1.529	1.543
C2–C3	1.518	1.523	1.517
C3–C4	1.525	1.519	1.514
C4–C5	1.541	1.540	1.533
C5–C10	1.559	1.559	1.562
C5–C6	1.535	1.535	1.537
C6–C7	1.529	1.529	1.531
C7–C8	1.533	1.534	1.539
C8–C9	1.555	1.551	1.543
C9–C10	1.564	1.564	1.555
C9–C11	1.545	1.541	1.536
C11–C12	1.539	1.538	1.537
C12–C13	1.533	1.538	1.534
C13–C14	1.543	1.548	1.543
C14–C8	1.530	1.531	1.525
C14–C15	1.535	1.529	1.521
C15–C16	1.554	1.546	1.546
C16–C17	1.553	1.560	1.553
C17–C13	1.553	1.562	1.555
C13–C18	1.541	1.542	1.535
C10–C19	1.543	1.543	1.536
C17–C20	1.553	1.548	1.538
C20–C21	1.537	1.534	1.525
C20–C22	1.543	1.544	1.544
C22–C23	1.540	1.539	1.534
C23–C24	1.509	1.509	1.503
C24=O	1.189	1.189	1.199
C24–O	1.328	1.328	1.325
O–CH_3	1.416	1.416	1.449
C3–OH	1.407	1.407	1.426

Table 3
Calculated (ab initio HF/6-31G*) and experimental (X-ray) bond angles (°) for MeLC

Bond angle (°)	Conformer 1	Conformer 2	X-ray structure
C1–C2–C3	110.4	110.4	110.0
C2–C3–C4	110.5	110.5	110.3
C2–C3–O3	107.8	112.1	111.9
O3–C3–C4	111.6	107.3	108.8
C3–O3–H	109.5	109.5	107.3
C3–C4–C5	113.0	112.9	111.9
C4–C5–C10	113.0	113.3	112.6
C4–C5–C6	110.9	110.8	111.8
C5–C6–C7	112.7	112.8	112.0
C6–C7–C8	112.1	112.1	112.0
C7–C8–C9	111.0	111.1	111.1
C8–C9–C10	112.5	112.7	112.7
C9–C10–C1	112.5	112.4	112.2
C7–C8–C14	111.7	111.6	110.9
C10–C9–C11	114.1	114.3	114.0
C9–C11–C12	113.6	113.7	112.8
C11–C12–C13	112.0	112.3	111.7
C12–C13–C14	107.6	106.6	106.8
C13–C14–C8	114.3	115.0	115.0
C8–C14–C15	119.9	119.0	118.9
C14–C15–C16	104.2	103.6	103.2
C15–C16–C17	105.9	107.2	107.3
C16–C17–C20	117.6	112.4	112.3
C13–C17–C20	119.2	120.0	119.9
C16–C17–C13	103.5	103.2	103.3
C17–C20–C22	115.9	109.5	108.8
C21–C20–C22	110.4	110.3	110.7
C17–C20–C21	109.7	113.3	113.4
C20–C22–C23	114.8	114.3	114.2
C22–C23–C24	113.4	111.2	111.1
C23–C24–O	112.0	112.0	112.1
C23–C24=O	125.1	125.0	125.1
O=C24–O	122.9	123.0	122.8
C24–O–CH_3	117.0	117.0	117.6

The calculations using the HyperChem software were run on Celeron 466 MHz PC.

Full geometry optimizations for a comparison with the conformational and structural properties obtained from the NMR and X-ray experiments were performed with the GAUSSIAN 98 series of programs [20] at the ab initio HF/6-31G* level of theory.

The absolute shieldings for MeLC and i-MeLC were obtained using the gauge-independent atomic orbital (GIAO) [21] method at the DFT B3LYP/6-311G* level of theory and HF/6-31G* optimized geometries. The predicted ^{13}C chemical shifts are derived from equation $\delta = \sigma_0 - \sigma$, where δ is the chemical shift, σ is the absolute shielding, and σ_0 is the absolute shielding of the standard (TMS in this case; 183.6 ppm [22]). In general, the DFT GIAO predictions are considered to provide reliable values with relatively small basis sets and with reasonable computational efforts. The calculations using the GAUSSIAN 98 program were run on Alpha 533 MHz PC.

2.4. X-ray crystallography

Single crystal of MeLC was grown by extremely slow evaporation from tetradeuteriomethanol solution. The X-ray structural data were collected with a Nonius Kappa CCD diffractometer at 173.0 ± 0.1 K

Table 4
Calculated (ab initio HF/6-31G*) and experimental (X-ray) dihedral angles (°) for MeLC

Dihedral angle (°)	Conformer 1	Conformer 2	X-ray structure
C1–C2–C3–C4	55.5	55.7	57.0
C2–C3–C4–C5	−55.5	−55.3	−57.8
C3–C4–C5–C6	−179.1	−179.2	−177.6
C4–C5–C6–C7	−72.9	−73.0	−71.1
C5–C6–C7–C8	−54.0	−53.9	−54.2
C6–C7–C8–C14	174.7	174.7	174.4
C7–C8–C14–C15	53.5	53.3	55.0
C8–C14–C15–C16	161.4	164.9	166.2
C14–C15–C16–C17	−4.3	−9.4	−11.7
C15–C16–C17–C13	−24.6	−19.3	−17.3
C16–C17–C13–C12	157.8	154.0	153.7
C17–C13–C12–C11	−164.6	−165.0	−166.2
C13–C12–C11–C9	53.4	54.7	56.8
C12–C11–C9–C10	179.6	178.7	177.1
C11–C9–C10–C1	−57.4	−58.2	−58.0
H–O–C3–C2	178.0	60.6	58.6
H–O–C3–C4	−60.6	−178.0	−179.2
O–C3–C2–C1	177.7	175.3	178.3
O–C3–C4–C5	−175.3	−177.8	179.1
C13–C17–C20–C22	−89.1	179.9	179.3
C13–C17–C20–C21	37.4	−58.5	55.7
C16–C17–C20–C22	145.8	56.4	−59.1
C16–C17–C20–C21	−87.8	177.9	177.2
C17–C20–C22–C23	167.2	169.3	173.1
C12–C13–C17–C20	−69.4	−80.0	−80.4
C15–C16–C17–C20	−158.4	−149.9	−148.0
C20–C22–C23–C24	−59.9	−175.6	−177.2
C22–C23–C24–O	−65.4	72.6	68.1
C23–C24–O–CH_3	180.0	−178.6	−176.9

using graphite monochromatized Mo^I Kα radiation (λ = 0.71073 Å). Data were processed with DENZO-SMN [23], the structure was solved by direct methods (SHELXS-97) [24] and refined on F^2 (SHELXL-97) [25]. The reflections were corrected for Lorenz polarization effects, absorption correction was not used. The hydrogen atoms were located from the difference Fourier map and refined with isotropic temperature factors (1.2–1.5 times the C temperature factor). Other experimental X-ray data are shown in Table 1. Crystallographic data (excluding structure factors) for the structure have been deposited with the Cambridge Crystallographic Data Center as supplementary publication No. CCDC-179240. Copies of the data can be obtained free of charge on application to CCDC, 12 Union Road, Cambridge CB2 1EZ, UK.

Unfortunately, all attempts to grow crystals of i-MeLC suitable for single crystal X-ray structural analysis failed although X-ray powder diffraction pattern revealed that the compound was crystalline.

3. Results and discussion

The molecular dynamics simulations led to two minimum energy conformations, which were further forwarded for semi-empirical PM3 and ab initio HF/6-31G* optimizations. The ab initio optimized structures of MeLC and i-MeLC are depicted in Figs. 2 and 3, respectively. ORTEP plot and crystal packing of MeLC are illustrated in Figs. 4 and 5, respectively. The structural parameters of the optimized conformations 1 and 2 of MeLC and its single crystal X-ray structure are compared in Tables 2–4. As can be seen, the calculated bond lengths and bond angles of MeLC equate very well with the X-ray structural parameters.

Table 5
Experimental ($CDCl_3$, 303 K) and DFT/B3LYP/6-311G* ^{13}C NMR chemical shifts of the two most stable gas phase conformers 1 and 2 of MeLC

C	δ_{exp}	δ_{calc} (1)	δ_{calc} (2)	δ_{calc} [(1)−(2)]	$\Delta\delta$ (1)	$\Delta\delta$ (2)	δ_{calc}	$\Delta\delta$
1	35.2	36.7	36.5	+0.2	−1.5	−1.3	36.5	−1.3
2	30.4	30.2	34.2	−4.0	+0.2	−3.8	34.0	−3.6
3	71.6	73.8	73.8	0.0	−2.2	−2.2	73.8	−2.2
4	36.3	40.9	36.0	+4.9	−4.6	+0.3	36.2	+0.1
5	42.0	45.9	45.7	+0.2	−3.9	−3.7	45.7	−3.7
6	27.1	29.7	29.3	+0.4	−2.6	−2.2	29.3	−2.2
7	26.3	28.5	28.3	+0.2	−2.2	−2.0	28.3	−2.0
8	35.7	38.5	39.0	−0.5	−2.8	−3.3	39.0	−3.3
9	40.3	43.8	43.8	0.0	−3.5	−3.5	43.8	−3.5
10	34.5	40.1	39.7	+0.4	−5.6	−5.2	39.7	−5.2
11	20.7	22.6	23.3	−0.7	−1.9	−2.6	23.3	−2.6
12	40.1	39.7	42.4	−2.7	+0.4	−2.3	42.3	−2.2
13	42.6	48.5	48.2	+0.3	−5.9	−5.6	48.2	−5.6
14	56.4	58.4	59.4	−1.0	−2.0	−3.0	59.3	−2.9
15	24.1	25.8	25.9	−0.2	−1.7	−1.8	25.9	−1.8
16	28.1	21.9	30.6	−8.6	+6.2	−2.5	30.2	−2.1
17	55.9	60.9	60.2	+0.8	−5.0	−4.3	60.2	−4.3
18	11.9	11.9	10.6	+1.3	0.0	+1.3	10.7	+1.2
19	23.3	23.0	22.7	+0.2	+0.3	+0.6	22.7	+0.6
20	35.3	31.1	42.4	−11.2	+4.2	−7.1	41.8	−6.6
21	18.2	20.2	16.6	+3.6	−2.0	+1.6	16.8	+1.4
22	30.9	31.3	35.3	−4.0	−0.4	−4.4	35.1	−4.2
23	30.9	34.9	36.1	−1.2	−4.0	−5.2	36.0	−5.1
24	174.6	172.4	172.7	−0.3	+2.2	+1.9	172.6	+2.0
25	51.3	48.5	48.8	−0.3	+2.8	+2.5	48.8	+2.5

The dihedral angles of the minimum energy conformation 2 of MeLC coincides very well with the corresponding parameters of the X-ray crystal structure (Figs. 2 and 4); the flexible side chain showing all-*trans* conformation as in crystalline CA [26]. On the other hand, in conformation 1 the side chain is in a *gauche* conformation about C22–C23 bond, which can be seen from the dihedral angle C20–C22–C23–C24 that is ca. 60°. In this form also the 3α-hydroxy group is oriented differently, the dihedral angle H–O–C3–C2 being 178.0° while in the X-ray structure it is 58.6°. A significant difference is also observed in the orientation of the side chain in respect of the cyclopentane ring. In conformation 1, the dihedral angle C13–C17–C20–C22 (−89.1°) is much smaller than the X-ray structural torsion angle (179.3°). Additionally, small differences in bending of cyclopentane ring between the two conformers 1 and 2 can be detected. However, in more rigid perhydrophenanthrene ring system of the steroid the calculated and experimental dihedral angles correspond relatively precisely.

According to the previously determined X-ray structures LCA [5] and DCA [27] both have a *gauche* side chain conformation in crystalline state. However, in LCA and DCA the side chain is *gauche* about the C20–C22-bond differing from the present crystal structure of MeLC, in which the *gauche* orientation is about the C22–C23-bond. In the *gauche* conformations of LCA and DCA both carboxylic oxygens are involved in hydrogen bonding, while in MeLC there exists only one hydrogen bond: 3α-O–**H**···**O**=C24, in which the distances O–H and H···O are 0.97(4) and 2.00(4) Å and the angle O–H···O is 170(3)°, respectively. There also exist significant differences between the crystal packing of LCA [5] and MeLC studied in this work. In its unit cell four LCA molecules are arranged in head-to-tail pairs with opposite orientations. In MeLC, the crystal packing (Fig. 5) is significantly tighter consisting of continuous parallel

Table 6
Calculated (ab initio HF/6-31G*) bond lengths (Å) for i-MeLC

Bond length (Å)	Conformer 1	Conformer 2
C1–C2	1.529	1.529
C2–C3	1.522	1.522
C3–C4	1.527	1.527
C4–C5	1.541	1.541
C5–C10	1.559	1.559
C5–C6	1.535	1.535
C6–C7	1.529	1.529
C7–C8	1.534	1.533
C8–C9	1.552	1.555
C9–C10	1.564	1.564
C9–C11	1.541	1.545
C11–C12	1.538	1.539
C12–C13	1.538	1.533
C13–C14	1.548	1.543
C14–C8	1.531	1.530
C14–C15	1.529	1.535
C15–C16	1.546	1.554
C16–C17	1.560	1.554
C17–C13	1.562	1.553
C13–C18	1.542	1.541
C10–C19	1.543	1.543
C17–C20	1.548	1.552
C20–C21	1.534	1.537
C20–C22	1.544	1.543
C22–C23	1.539	1.539
C23–C24	1.508	1.508
C24=O	1.189	1.189
C24–O	1.328	1.328
O–CH_3	1.416	1.416
C3–OH	1.411	1.411

Table 7
Calculated (ab initio HF/6-31G*) bond angles (°) for i-MeLC

Bond angle (°)	Conformer 1	Conformer 2
C1–C2–C3	111.2	111.2
C2–C3–C4	110.5	110.6
C2–C3–O3	107.1	107.1
O3–C3–C4	111.7	111.7
C3–O3–H	109.4	109.4
C3–C4–C5	113.6	113.6
C4–C5–C10	113.1	113.1
C4–C5–C6	110.7	110.7
C5–C6–C7	112.9	112.8
C6–C7–C8	112.2	112.2
C7–C8–C9	111.2	111.1
C8–C9–C10	112.8	112.5
C9–C10–C1	112.6	112.7
C7–C8–C14	111.6	111.7
C10–C9–C11	114.3	114.1
C9–C11–C12	113.7	113.6
C11–C12–C13	112.3	112.0
C12–C13–C14	196.6	107.6
C13–C14–C8	115.0	114.3
C8–C14–C15	119.0	120.0
C14–C15–C16	103.6	104.2
C15–C16–C17	107.2	106.0
C16–C17–C20	112.3	117.3
C13–C17–C20	120.0	119.0
C16–C17–C13	103.2	103.7
C17–C20–C22	109.5	115.4
C21–C20–C22	110.2	110.2
C17–C20–C21	113.3	109.6
C20–C22–C23	114.3	112.8
C22–C23–C24	110.9	111.6
C23–C24–O	111.8	111.9
C23–C24=O	125.1	125.0
O=C24–O	123.1	123.0
C24–O–CH_3	117.0	117.0

hydrogen bonded (3α-O**H**···**O**=C24) head-to-tail polymeric chains. Further, these chains are cross-linked by many simultaneous weak interactions OC(sp^3)**H**···**O**H, characterized by **C**(sp^3)–**O** distance of 2.993(0.003) Å and a **C**(sp^3)–**H**–**O** angle of 96.7(2.0)°. The short C–O-distance suggests that this interaction could be a weak hydrogen bond while its C–H–O directionality favors its interpretation as van der Waals interaction by character [28]. However, this exceptionally tight crystal packing, in which many simultaneous weak interactions play a crucial role, can explain the difficulties in getting single crystals suitable for X-ray structural analyses from bile acid esters.

In i-MeLC the energetically most stable gas phase conformer resembles the X-ray structure of MeLC (except, of course, the orientation of 3-OH moiety). Also the higher energy conformers of MeLC and i-MeLC are quite similar, however, in i-MeLC the side chain possesses a slightly more folded structure. Additionally, in i-MeLC the two low energy conformers show very similar structural parameters in the steroidal skeleton (including 3β-OH). Actually, the only difference can be observed in the conformations of the side chains. Unfortunately, all attempts to grow suitable crystals for single crystal X-ray structural analysis of i-MeLC failed. In powder X-ray diffraction experiments i-MeLC crystals gave nice diffraction patterns.

Table 8
Calculated (ab initio HF/6-31G*) dihedral angles (°) for i-MeLC

Dihedral angle (°)	Conformer 1	Conformer 2
C1–C2–C3–C4	53.8	53.8
C2–C3–C4–C5	−53.7	−53.7
C3–C4–C5–C6	−179.7	−179.7
C4–C5–C6–C7	−72.9	−73.0
C5–C6–C7–C8	−53.7	−53.8
C6–C7–C8–C14	174.7	174.6
C7–C8–C14–C15	53.2	53.5
C8–C14–C15–C16	164.9	162.1
C14–C15–C16–C17	−9.4	−5.3
C15–C16–C17–C13	−19.3	−23.6
C16–C17–C13–C12	154.0	157.2
C17–C13–C12–C11	−165.0	−164.7
C13–C12–C11–C9	54.7	53.4
C12–C11–C9–C10	178.8	179.6
C11–C9–C10–C1	−58.1	−57.1
H–O–C3–C2	179.9	180.0
H–O–C3–C4	58.7	58.8
O–C3–C2–C1	−68.1	−68.1
O–C3–C4–C5	65.4	65.4
C13–C17–C20–C22	179.9	−88.1
C13–C17–C20–C21	56.4	146.9
C16–C17–C20–C22	−58.5	38.1
C16–C17–C20–C21	177.9	−86.9
C17–C20–C22–C23	170.0	159.2
C12–C13–C17–C20	−80.0	−70.4
C15–C16–C17–C20	−150.0	−157.0
C20–C22–C23–C24	−172.5	178.1
C22–C23–C24–O	−73.8	70.2
C23–C24–O–CH_3	178.5	−178.8

However, the crystal data and structural parameter determination have been unsuccessful so far.

The assignments of ^{13}C NMR chemicals shifts of MeLC and i-MeLC are based on PFG ^{1}H, ^{13}C HMQC and ^{13}C DEPT-135 runs and are in agreement with the literature data [29,30]. The energy difference between the two most stable gas phase conformers of MeLC was only 6.9 kJ mol^{-1} (1.7 kcal mol^{-1}). According to Boltzmann distribution, the contribution of the higher energy conformation to the conformational equilibrium is low, only 4.6%. The same is true for i-MeLC, in which the corresponding energy difference was 6.4 kJ mol^{-1} (1.5 kcal mol^{-1}) resulting to a contribution of the higher energy conformation to the overall conformational equilibrium of 5.7%. In order to achieve as accurate results as possible the theoretical ^{13}C NMR chemical shifts for the two low energy conformers of α- (MeLC) as well as β-epimers (i-MeLC) were calculated and the theoretical ^{13}C NMR chemical shifts defined using weighted averages, although it doubled the CPU time needed.

Linear regression analysis between the experimental ^{13}C NMR chemical shifts of MeLC, δ_{exp}, measured in deuteriochloroform and the weighted average values of the DFT/B3LYP calculated chemical shifts for the two most stable gas phase conformers 1 and 2, δ_{calc}, gives the following relationship (1):

$$\delta_{calc}[^{13}C(i)_{MeLC}] = 0.981\delta_{exp}[^{13}C(i)_{MeLC}] + 3.026 \text{ ppm}, \quad (1)$$

with multiple $R = 0.997$, number of carbons = 25, standard error = 2.4 ppm.

A comparable Eq. (2) was obtained for i-MeLC:

$$\delta_{calc}[^{13}C(i)_{i\text{-}MeLC}] = 0.986\delta_{exp}[^{13}C(i)_{i\text{-}MeLC}] + 2.972 \text{ ppm}, \quad (2)$$

with multiple $R = 0.997$, number of carbons = 25, standard error = 2.5 ppm.

A general equation for monomeric bile acid esters (Eq. (3)) can be presented by doing linear regression analysis between the experimental and the weighted average values of the DFT/B3LYP calculated chemical shifts for both epimers:

$$\delta_{calc}[^{13}C(i)] = 0.984\delta_{exp}[^{13}C(i)] + 3.000 \text{ ppm}, \quad (3)$$

with multiple $R = 0.997$, number of carbons = 50, standard error = 2.4 ppm.

The constant term can be regarded as an average difference of the bulk shielding effects of the solvent on the solute and reference (TMS) molecules. This argument is supported by inspecting the shift differences, $\Delta\delta$, of the methyl carbons C18, C19, and C21 of MeLC and i-MeLC (see Tables 5 and 9) where the solvent environment resembles probably most the circumstances around the methyl groups of TMS. As can be seen the $\Delta\delta$ values are +1.2 (Me-18), +0.6 (Me-19), and +1.4 ppm (Me-21) for MeLC and +1.2 (Me-18), +0.6 (Me-19), and +1.6 ppm (Me-21) for i-MeLC, respectively, being part of the group of the smallest differences in the whole set of chemical shifts. This finding gives one way to estimate the accuracy of the results of the theoretical calculations and an extra reason to perform the often

Table 9
Experimental ($CDCl_3$, 303 K) and DFT/B3LYP/6-311G* ^{13}C NMR chemical shifts of the two most stable gas phase conformers 1 and 2 of i-MeLC

C	δ_{exp}	δ_{calc} (1)	δ_{calc} (2)	δ_{calc} [(1)−(2)]	$\Delta\delta$ (1)	$\Delta\delta$ (2)	δ_{calc}	$\Delta\delta$
1	29.7	30.5	30.9	−0.4	−0.8	−1.2	30.5	−0.8
2	27.6	27.9	28.1	−0.2	−0.3	−0.5	27.9	−0.3
3	66.7	69.4	69.1	+0.3	−2.7	−2.4	69.4	−2.7
4	33.3	38.4	38.3	+0.1	−5.1	−5.0	38.4	−5.1
5	36.3	39.9	40.1	−0.2	−3.6	−3.8	39.9	−3.6
6	26.5	28.9	29.1	−0.2	−2.4	−2.6	28.9	−2.4
7	26.1	28.4	28.5	−0.1	−2.3	−2.4	28.4	−2.3
8	35.5	38.9	38.4	+0.5	−3.4	−2.9	38.9	−3.4
9	39.6	43.4	43.6	−0.2	−3.8	−4.0	43.4	−3.8
10	34.9	40.5	41.1	−0.6	−5.6	−6.2	40.5	−5.6
11	20.9	23.4	22.9	+0.5	−2.5	−2.0	23.4	−2.5
12	40.1	42.4	39.9	+2.5	−2.3	+0.2	42.3	−2.2
13	42.6	48.2	48.4	−0.2	−5.6	−5.8	48.2	−5.6
14	56.4	59.6	58.5	+1.1	−3.2	−2.1	59.5	−3.1
15	24.0	25.8	25.9	−0.1	−1.8	−1.9	25.8	−1.8
16	28.0	30.5	21.9	+8.6	−2.5	+6.1	30.0	−2.0
17	55.8	60.2	60.7	−0.5	−4.4	−4.9	60.2	−4.4
18	11.9	10.6	12.2	−1.6	+1.3	−0.3	10.7	+1.2
19	23.7	23.1	23.2	−0.1	+0.6	+0.5	23.1	+0.6
20	35.1	42.1	34.3	+7.8	−7.0	+0.8	41.7	−6.6
21	18.1	16.2	20.9	−4.7	+1.9	−2.8	16.5	+1.6
22	30.8	35.1	32.8	+2.3	−4.3	−2.0	35.0	−4.2
23	30.8	36.3	36.6	−0.3	−5.5	−5.8	36.3	−5.5
24	174.5	173.3	172.4	+0.9	+1.2	+2.1	173.2	+1.3
25	51.2	48.7	48.8	−0.1	+2.5	+2.4	48.7	+2.5

CPU time invasive procedures in order to estimate the solvent effects in different parts of the molecule. Other shifts estimated reasonably precisely by this method are the A-ring carbons C1 and C4 for MeLC, C1 and C2 for i-MeLC, as well as the D-ring carbon C15 for both epimers. The $\Delta\delta$ ^{13}C chemical shift C24 for the β-epimer was +1.3 ppm, being of the same range as the $\Delta\delta$ for the methyl groups.

On the other hand, the maximum $\Delta\delta$ values for MeLC are −5.2 (C10), −5.6 (C13), and −6.6 ppm (C20) and for i-MeLC −5.6 (C10), −5.6 (C13), and −6.6 ppm (C20). The chemical shift of carbon C17 also shows large deviations from the experimental values $\Delta\delta$ being −4.3 ppm for MeLC and −4.4 ppm for i-MeLC, respectively. All the previously mentioned carbon atoms are bearing an alkyl substituent. Carbons C10 and C13 are in addition located in the interior of the molecule. Also the chemical shifts of the side chain carbons C22 and C23 differ markedly from the experimental values, $\Delta\delta$ being −4.2 and −5.1 ppm for MeLC and −4.2 and −5.5 ppm for i-MeLC, respectively. Interestingly, the chemical shift of an A-ring carbon C4 for i-MeLC also deviates quite a lot from the experimental value, −5.1 ppm. Consequently, the differences cannot be explained by solvent effects but merely by the inability of the calculational procedure to reproduce the ^{13}C NMR chemical shifts for those particular carbons.

These three methods for predicting a molecular structure all work in different phases; X-ray crystallography in solid phase, NMR spectroscopy in solution phase, and molecular modeling in gas phase. In solid phase, the influences of crystal packing affect the structure and orientation of the molecules as described earlier. In solution, the solvation as well as the other thermodynamic equilibria play crucial roles influencing the values of the chemical shifts. Molecular modeling calculations, however, are usually performed in vacuo. That is why it is astonishing to observe how well data from different sources

correspond. This is most probably due to the relatively rigid polycyclic ring system of steroids. The assumption is supported by examining the side chain carbon atoms, for which the deviations between the experimental and theoretical values are the largest. In determining different structural parameters for steroidal molecules, these three methods can be used in parallel concerning the limitations of each one separately.

4. Conclusions

An exceptionally tight crystal packing of MeLC reveals interesting features, which can explain the difficulties in growing single crystals suitable for X-ray structural analysis from bile acid esters. The strong hydrogen bonded (O**H**···**O**=C24) continuous head-to-tail polymeric chains of MeLC molecules in crystals are further cross-linked by several simultaneous weak C(sp^3)**H**···**O** type of interactions, which fall between the categories of weak hydrogen bonds and van der Waals contacts. The molecular structure of MeLC in crystalline state equates very well with the other of the two predominant conformers in gas phase screened by molecular modeling. Excellent linear relationships between experimental and DFT/GIAO calculated ^{13}C NMR chemical shifts for both MeLC and i-MeLC (epimer of MeLC) show that novel calculational GIAO methods at the level of density functional theory (DFT) can reproduce ^{13}C NMR chemical shifts for steroids with reasonable computational time and resources.

Acknowledgements

The authors wish to thank Spec. Lab. Technician Reijo Kauppinen for his help in running the NMR spectra. Mr Juha Linnanto is acknowledged for valuable comments. E.V. gratefully acknowledges the Faculty of Mathematics and Science of University of Jyväskylä and the Foundation of Magnus Ehrnrooth for financial support.

References

[1] P.P. Nair, D. Kritchevsky, in: D. Kritchevsky, P.P. Nair (Eds.), The Bile Acids. Chemistry, Physiology and Metabolism, Plenum Press, New York, 1971, Chapter 1.
[2] J.R. Dias, H. Gao, E. Kolehmainen, Spectrochim. Acta A56 (2000) 53 and references cited therein.
[3] M. Sugahara, S. Kazuki, H. Junji, M. Miyata, Mol. Cryst. Liq. Cryst. Sci. Technol., Sect. A 356 (2001) 155 and references cited therein.
[4] D.A. Norton, B. Haner, Acta Cryst. 19 (1965) 478.
[5] S.K. Arora, G. Germain, J.P. Declercq, Acta Cryst. B32 (1976) 415 and references cited therein.
[6] W.B. Smith, Magn. Reson. Chem. 37 (1999) 103 and references cited therein.
[7] J. Tamminen, E. Kolehmainen, Molecules 6 (2000) 21.
[8] J. Tamminen, E. Kolehmainen, M. Haapala, J. Linnanto, Synthesis (2000) 1464.
[9] E. Kolehmainen, M. Kaartinen, R. Kauppinen, J. Kotoneva, K. Lappalainen, Magn. Reson. Chem. 32 (1994) 441.
[10] J. Tamminen, E. Kolehmainen, M. Haapala, H. Salo, J. Linnanto, ARKIVOC 1 (2000) 90.
[11] D. Albert, M. Feigel, Tetrahedron Lett. 35 (1994) 565.
[12] D. Albert, M. Feigel, Helv. Chim. Acta 80 (1997) 2168.
[13] F.C. Chang, J. Org. Chem. 44 (1979) 4567.
[14] A. Bax, S. Subramanian, J. Magn. Reson. 67 (1986) 565.
[15] A. Bax, M.F. Summers, J. Am. Chem. Soc. 108 (1986) 2093.
[16] HyperChem™, Version 4.5 for Windows, Hypercube, Inc., Waterloo, Canada, 1994.
[17] N.L. Allinger, J. Am. Chem. Soc. 99 (1977) 8127.
[18] N.L. Allinger, Y.H. Yuh, Quantum chemistry program exchange, Bloomington, Indiana, Program No. 395, molecular mechanics, in: U. Burkert, N.L. Allinger (Eds.), ACS Monograph 177, American Chemical Society, Washington, DC, 1982.
[19] J.J.P. Stewart, J. Comput. Chem. 10 (1989) 209.
[20] M.J. Frisch, G.W. Trucks, H.B. Schlegel, G.E. Scuseria, M.A. Robb, J.R. Cheeseman, V.G. Zakrzewski, J.A. Montgomery Jr., R.E. Stratmann, J.C. Burant, S. Dapprich, J.M. Millam, A.D. Daniels, K.N. Kudin, M.C. Strain, O. Farkas, J. Tomasi, V. Barone, M. Cossi, R. Cammi, B. Mennucci, C. Pomelli, C. Adamo, S. Clifford, J. Ochterski, G.A. Petersson, P.Y. Ayala, Q. Cui, K. Morokuma, P. Salvador, J.J. Dannenberg , D.K. Malick, A.D. Rabuck, K. Raghavachari, J.B. Foresman, J. Cioslowski, J.V. Ortiz, B.B. Stefanov, G. Liu, A. Liashenko, P. Piskorz, I. Komaromi, R. Gomperts, R.L. Martin, D.J. Fox, T. Keith, M.A. Al-Laham, C.Y. Peng, A. Nanayakkara, C. Gonzalez, M. Challacombe, P.M.W. Gill, B. Johnson, W. Chen, M.W. Wong, J.L. Andres, C. Gonzalez, M. Head-Gordon, E.S. Replogle, J.A. Pople, GAUSSIAN98, Revision A.11, Gaussian, Inc., Pittsburgh, PA, 2001.
[21] K. Wolinski, J.F. Hilton, P.J. Pulay, J. Am. Chem. Soc. 112 (1990) 8251.
[22] E. Kolehmainen, J. Koivisto, V. Nikiforov, M. Peräkylä, K. Tuppurainen, K. Laihia, R. Kauppinen, S.A. Miltsov, V.S. Karavan, Magn. Reson. Chem. 37 (1999) 743.

[23] Z. Otwinowski, W. Minor, in: C.W. Carter Jr., R.M. Sweet (Eds.), Macromolecular Crystallography, Part A, Methods of Enzymology, vol. 276, Academic Press, New York, 1997, pp. 307–326.
[24] G.M. Sheldrick, Acta Cryst. A46 (1990) 467.
[25] G.M. Sheldrick, SHELXL-97™A Program for Crystal Structure Refinement, University of Göttingen, Germany, 1997.
[26] P.L. Johnson, J.P. Schaefer, Acta Cryst. B28 (1972) 3083.
[27] S. Candeloro de Sanctis, E. Giglio, V. Pavel, C. Quagliata, Acta Cryst. B28 (1972) 3656.
[28] T. Steiner, G.R. Desiraju, Chem. Commun. (1998) 891.
[29] J.W. Blunt, J.B. Stothers, Org. Magn. Reson. 9 (1977) 439.
[30] T. Iida, T. Tamura, T. Matsumoto, F.C. Chang, Org. Magn. Reson. 21 (1983) 305.